#### RESEARCH ARTICLE



## Fabrication and characterization of gold nanospheres-cored pH-sensitive thiol-ended triblock copolymer: A smart drug delivery system for cancer therapy

#### Correspondence

Farideh Mahmoodzadeh, Halal Research Center of IRI, FDA, Tehran, Iran. Email: mahmoodzadeh.farideh@gmail.com

Marjan Ghorbani, Stem Cell Research Center, Tabriz University of Medical Sciences, Tabriz,

Email: ghorbani.marjan65@yahoo.com

Conventional chemotherapy suffers lack of multidrug resistance (MDR), lack of bioavailability, and selectivity. Nano-sized drug delivery systems (DDS) are developing aimed to solve several limitations of conventional DDS. These systems have been offered for targeting tumor tissue owing to enhanced long circulation time, drug solubility, their retention effect, and improved permeability. As a result, the aim of this project was the design and development of DDS for biomedical applications. For this purpose, gold nanospheres (GNSs) covered by pH-sensitive thiol-ended triblock copolymer [poly(methacrylic acid) -b-poly(acrylamide) -b-poly(ε-caprolactone)-SH; PMAA-b-PAM-b-PCL-SH] for delivery of anticancer drug doxorubicin (DOX). The chemical structures of triblock copolymer were investigated by proton nuclear magnetic resonance (<sup>1</sup>H NMR) and Fourier transform infrared (FTIR) spectroscopies. <sup>1</sup>H NMR spectroscopy and gel permeation chromatography (GPC) were used for calculating the molecular weights of each part in the nanocarrier. The success of coating, GNSs with triblock copolymer was considered by means of dynamic light scattering (DLS), FTIR, ultraviolet-visible (UV-Vis), and transmission electron microscopy (TEM) measurement. The pH-responsive drug release ability, (DOX)-loading capacity, biocompatibility, and in vitro cytotoxicity effects of the nanocarriers were also studied. As a result, it is expected that the synthesized GNSs@polymer-DOX considered as a potential application in nanomedicine demand like smart drug delivery, imaging, and chemo-photothermal therapy.

#### **KEYWORDS**

gold nanospheres, pH-responsive, polymeric micelles, RAFT polymerization, smart drug delivery

#### 1 | INTRODUCTION

Cancer is a large group of disease in the earth, which induce the patient death.

Patients are most usually treated with surgery, radiation therapy, and chemotherapy. 1,2 Among them, chemotherapy is a common therapeutic technique for the treatment of numerous cancers. Nevertheless, nonspecific delivery of anticancer agents leads to harmful and adverse side effects on human normal cells and inadequate dosages

to kill cancer cells.<sup>3,4</sup> So, to overcome these problems, nanoscale drug delivery systems (DDS) such as polymeric micelles<sup>5-8</sup> have achieved remarkable consideration, in the field of cancer therapy because of their self-assembly ability in the aqueous solvent upon responding to external stimuli initiates, for example, temperature, special enzymes, ionic light, pH, and electric field. 9-12 Various nanomicelles containing nanorods, vesicles, core-shell-corona nanospheres, and multicompartment nanoparticles have been arranged, depending on the process of micellization, solvent character, and

<sup>&</sup>lt;sup>1</sup>Halal Research Center of Islamic Republic of Iran, Food and Drug Administration, Tehran, Iran

<sup>&</sup>lt;sup>2</sup>Marand Faculty of Technical and Engineering, University of Tabriz, Tabriz, Iran <sup>3</sup>Stem Cell Research Center, Tabriz University of Medical Sciences, Tabriz, Iran

copolymer structure.<sup>13,14</sup> Among the various shape, core-shell-corona nanospheres organized from triblock copolymers are less considered, essentially owing to complex structures and trouble in the production of micelles.<sup>15,16</sup>

The pH-responsive polymeric micelles have been used for targeting drug delivery to tumors because of their stability at physiological pH and water solubility, As well as, these types of polymers like polyacrylic acid can either accept protons in cancer tissue because of the external pH of cancerous tissue tends to be lower in evaluation with the surrounding normal tissue. 17-20 Among the various methods for the synthesis of polymeric micelles, "living" radical polymerization is important. This method is separated into three main class, namely, atom transfer radical polymerization (ATRP), 21,22 reversible additionfragmentation chain transfer (RAFT) polymerization, 13,23 and nitroxide-mediated polymerization (NMP).<sup>24,25</sup> Mentioned methods have been established as useful methods to prepare polymeric materials with complex macromolecular and well-defined structural. Among them, the RAFT procedure has developed very interesting because of its applicability to various vinyl monomers and its applicability for preparation of block copolymers and homopolymers with controlled molecular weight.<sup>26-28</sup> Furthermore, by chemical reduction techniques, the synthesized macromolecules via RAFT polymerization method can be produced a thiol group.

The thiol-ended copolymer has a strong attraction towards metal nanoparticle like gold nanospheres (GNSs) via the creation of Au–S bond. In new year's, polymer modified GNSs have been attained a tremendous attention in bioanalytical (eg, biosensors)<sup>29</sup> and biomedical (eg, diagnosis and drug delivery)<sup>6</sup> fields. This intense attention created from biological features as well as superior physicochemical of GNSs including low cytotoxicity, good biocompatibility, excellent chemical stability, and enhance the transfection efficiency.<sup>30,31</sup>

The aim of this project is the fabrication and characterization of GNSs-cored pH-sensitive thiol-ended triblock copolymer as a smart DDS for cancer therapy. For this reason, GNSs-modified polymeric micelles were synthesized by covering GNSs with pH-responsive thiol-end-capped triblock copolymer [poly(methacrylic acid) -b-poly(acrylamide) -b-poly(\varepsilon-caprolactone)-SH; PMAA-b-PAM-b-PCL-SH]. Additionally, the anticancer drug doxorubicin (DOX) was attached onto the GNSs-modified polymers (GNSs@polymer) by the electrostatic force and the nanocarriers prepared were named GNSs@polymer-DOX. The chemical structures, the success of coating triblock copolymer, pH-responsive drug release ability, biocompatibility, in vitro cytotoxicity effects of the nanocarriers, and (DOX)-loading capacity were also studied.

#### 2 | EXPERIMENTAL

#### 2.1 | Materials

The (CTA-PCL-S)<sub>2</sub> macro-RAFT agent was prepared in our laboratory.<sup>5</sup> The initiator of 2,2-azobisisobutyronitrile (AIBN; Fluka, Switzerland) was recrystallized in absolute ethanol at 55°C. Dithiothreitol (DTT),

sodium citrate ( $Na_3C_6H_5O_7.2H_2O$ , more than 99%), hydrochloroauric acid trihydrate ( $HAuCl_4.3H_2O$ , 99.9%), and sodium methoxide were purchased from Merck and were used as accepted. Methacrylic acid monomer (Sigma-Aldrich) was distilled in reduced pressure. The acrylamide (AM) monomer was purchased from Merck. DOX hydrochloride was donated from Zahravi Company and used as obtained. Methyl thiazolyl tetrazolium (MTT) (3-(4, 5-dimethylthiazol-2-yl)-2,5-diphenyltetrazolium bromide), fetal bovine serum, and other biological reagents were purchased from Invitrogen (Carlsbad, CA, USA) and were used as received. All other chemicals were obtain from Sigma-Aldrich or Merck and purified as reported by standard methods.

# 2.2 | Preparation of (PAM-b-PCL-S)<sub>2</sub> triblock copolymer

A dry flask was charged with AM (7 mmol, 0.5 g), (CTA PCL-S)<sub>2</sub> macro-RAFT agent (0.12 mmol, 1.56 g), AIBN (12  $\mu$ mol, 2.0 mg), and N,N-dimethylformamide (DMF, 6 mL). The content of flask was stirred for about 1 day at 70°C under argon atmosphere. Then, to quench the reaction, the flask was cooled in ice/water. The content of the flask was poured in excess of cold diethyl ether, filtered, and washed several times with diethyl ether. The product was dried under reduced pressure at 25°C.

# 2.3 | Preparation of (PMAA-b-PAM-b-PCL-S)<sub>2</sub> pentablock copolymer

MAA monomer (0.86 g, 10 mmol), DMF (6 mL), the (PAM-b-PCL-S)<sub>2</sub> macro-RAFT agent (0.06 mmol, 1.38 g), and AIBN (12  $\mu$ mol, 2.0 mg) were dissolved in a dried polymerization ampoule under argon atmosphere. Then, the ampoule was placed in an oil bath at 70°C for about 1 day. After this time, to quench the reaction, the ampoule was cooled in ice/water. The content of the flask was poured in excess of cold diethyl ether, filtered, and washed three times with diethyl ether. The product was dried under reduced pressure at 25°C.

# 2.4 | Preparation of PMAA-b-PAM-b-PCL-SH triblock copolymer

According to the literature, chemical reduction of disulfide band via DTT is a promising method for preparation of thiol end-capped polymers. For this purpose,  $CH_3ONa$  (0.044 mmol, 2.4 mg), DTT (1.0 mmol, 0.15 g), and (PMAA-b-PAM-b-PCL-S) $_2$  (0.035 mmol, 1.44 g) were dissolved in dried tetrahydrofuran (THF). The reaction was allowed to proceed for 2 days at 25°C under argon protection. To obtain the precipitate and prevent disulfide formation, the product dropped into a 300 mL of degassed diethyl ether. The mixture obtained was filtered and dried under vacuum at 25°C.

#### 2.5 | PMAA-b-PAM-b-PCL-SH micelle formation

A total of 40-mg (PMAA-b-PAM-b-PCL-SH) triblock copolymer was dissolved in 8-mL DMSO to obtain a polymer solution. Then, the solution was dialyzed against deionized (DI) water for 2 days with strong stirring. In first 4 hours, the media changed once per hour. The solution consist of PMAA-b-PAM-b-PCL-SH transformed from transparent to translucent over the dialysis, which establishes the production of polymeric micelles.

## 2.6 | Preparation of GNSs

GNSs were prepared by standard citrate reduction method. 32,33 Briefly, after boiling the aqueous solution of HAuCl<sub>4</sub> (0.5mM, 100 mL), sodium citrate aqueous solution (1 wt%, 5 mL) was added under strong stirring. The reaction was allowed to proceed for 20 minutes. After this time, reaction color changed from light yellow to wine red established the creation of GNSs (Figure 1).

#### 2.7 | Preparation of GNSs@polymer

The GNSs@polymer nanocarriers were produced via the fabrication of Au–S bond between the resulting thiol end-capped polymer and GNSs as follows.

A total of 50-mg (PMAA-b-PAM-b-PCL-SH) triblock copolymer was dissolved in 10-mL DMSO to obtain polymer solution, and then 5-mL aqueous solution of GNSs (3 mg mL<sup>-1</sup>) was little by little added into the polymer solution under strong stirring. To complete the ligand exchange, the solution was kept under stirring for 1 day. At the end of this time, in order to remove free polymeric chains, GNSs@polymer was dialyzed against DI water for about 72 hours. The solution containing GNSs@polymer transformed from transparent red to cloudy red over the dialysis, which establish the production of Au-S bond.<sup>11</sup>

## 2.8 | Synthesis of GNSs@polymer-DOX

GNSs@polymer (50-mg nanocomposite in 5-mL deionized water) and DOX (5 mg) were transferred in a 50-ml dark flask. To obtain the high drug loading content, the reaction mixture was mixed for about 48 hours

at 25°C. At the end of this time, the GNSs@polymer-DOX was collected by centrifugation at 12 000 rpm approximately 10 minutes. By the measuring unloaded drug concentration via UV-Vis spectroscopy, the DOX-encapsulation efficiency of the GNSs@polymer was measured as 94.63% by using the following equation.<sup>28</sup>

$$\mathsf{EE}(\%) = \frac{(C_T - C_{DOX})}{C_T} \times 100,$$

C<sub>DOX</sub>: DOX concentration in supernatant solution;

C<sub>T</sub>: DOX total concentration, which used for loading.

## 2.9 | In vitro release study

GNSs@polymer-DOX (10 mg) was suspended in phosphate buffered saline (PBS) and then transferred into a dialysis bag (cutoff molecular weight 12 000 g mol<sup>-1</sup>). The bags were placed in 40 mL of (PBS) solutions at pH values of 7.4, 5.4, and 4.0. For studying the amount of released DOX using UV-Vis spectrophotometer, 1 mL of release medium was collected at predetermined time intervals. It is important to note that, to sustain the equal total solution volume, 1 mL of the release medium was brought back into the container. The amounts of Dox release were analyzed via the standard calibration curve.<sup>28,34</sup>

#### 2.10 | Cell culture

MCF7 breast cancer cell line was purchase from National Cell Bank of Iran and cultivated in Roswell Park Memorial Institute 1640 medium including 100 IU penicillin per 100- $\mu$ g streptomycin, supplemented with 10% (v/v) of fetal bovine serum. The cells were cultured into flasks and kept in a humidified atmosphere with 5% CO<sub>2</sub> at 37°C, and the media refreshed twice weekly.<sup>35</sup>

## 2.11 | Cell viability assay

Cell viability was performed using a colorimetric MTT assay. Human breast adenocarcinoma MCF-7 cells was trypsinized, harvested, and seeded in 96 well plates. After 20-hour incubation, the cells were treated with different concentrations of GNSs-citrate, GNSs@polymer, and GNSs@polymer-DOX for 48 hours. After 48 hours, the media









**FIGURE 1** The image of change color (left to right) during the formation of gold nanospheres (GNSs) [Colour figure can be viewed at wileyonlinelibrary.com]

containing samples was removed, and 200 µL of MTT solution were then added to each well. After the incubation for an additional 4 hours, the medium containing remaining MTT was removed carefully from wells. To dissolve the formed formazan crystals, 150 µL of dimethyl sulfoxide was added to each well. The absorbance of solubilized formazan was measured at 570 nm by spectrophotometric plate reader, ELx800 (Biotek, San Francisco, CA, USA). All tests were done in triplicate. 36,37

#### 2.12 | Characterization

Proton nuclear magnetic resonance (<sup>1</sup>H NMR) spectra were verified at 25°C using <sup>1</sup>H NMR (400 MHz) Bruker spectrometer (Ettlingen, Bruker, Germany). Fourier transform infrared (FTIR) spectra of the samples were recorded by Shimadzu 8101M FTIR (Kyoto, Shimadzu, Japan) at the wavenumber ranges from 400 to 4000 cm<sup>-1</sup>.

The molecular weights of samples were examined by gel permeation chromatography (GPC) with a Maxima 820 GPC Analysis Report (Ventura, CA, USA).

THF were used as eluent at a flow rate of 1 mL min<sup>-1</sup> and column temperature of 25°C.

Ultraviolet-visible (UV-Vis) spectroscopy was planned by a Shimadzu 1650 PC UV-Vis spectrophotometer (Shimadzu, Kyoto, Japan).

Transmission electron microscopy (TEM) was performed on a Philips CM10-TH microscope (The Netherlands, Eindhoven, Phillips) at an accelerating voltage of 100 kV. Dynamic light scattering (DLS) was planned through a laser-scattering method (Malvern, Zetasizer Nano ZS90, UK) at different pH values.

#### 3 | RESULTS AND DISCUSSION

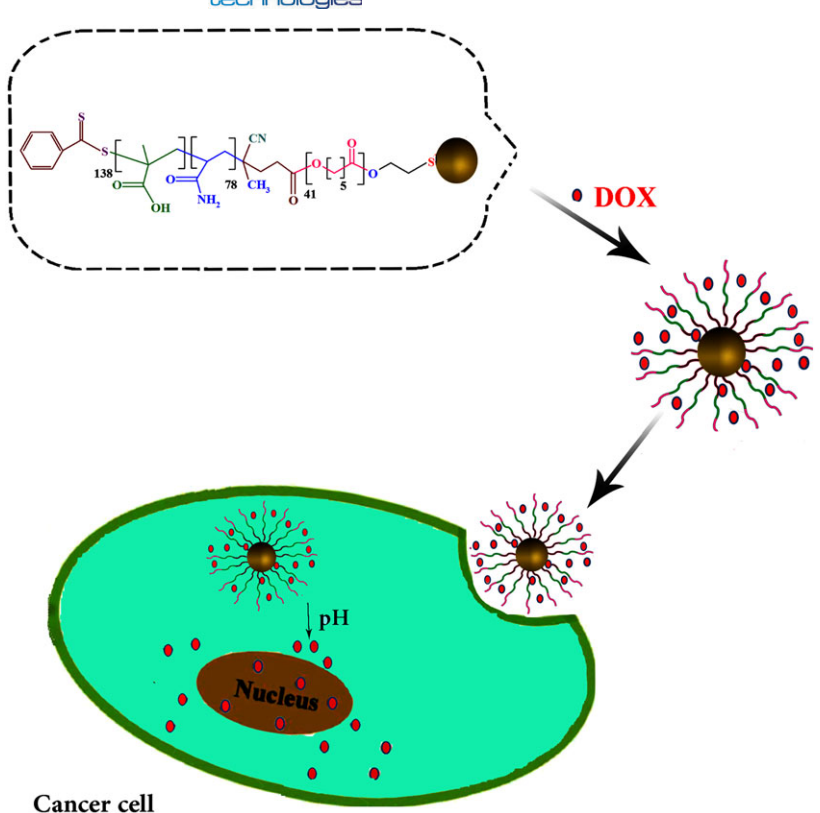
As demonstrated in Schemes 1 and 2, we aim to provide a novel smart DDS for cancer therapy. For this purpose, GNSs covered by pH-sensitive thiol-ended triblock copolymer [poly(methacrylic acid) b-poly(acrylamide) -b-poly(e-caprolactone)-SH: PMAA-b-PAM-b-PCL-SH] for delivery of anticancer drug DOX. This nanosystem could be used for theranostic applications and chemo-photothermal therapy because of optical absorption in the near-infrared region (NIR) and conversion of absorbed light into local heating.

## 3.1 | Evaluation of PMAA-b-PAM-b-PCL-SH triblock copolymer

## 3.1.1 | FTIR and <sup>1</sup>H NMR spectroscopies

As demonstrated in Figures 2 and 3, <sup>1</sup>H NMR and FTIR spectroscopies were used to describe the PMAA-b-PAM-b-PCL-SH triblock copolymer. The most important bands in the FTIR spectrum of the (CTA-PCL-S)<sub>2</sub> sample (Figure 2A) can be listed as the stretching vibration of carbonvl group at 1724 cm<sup>-1</sup>, the bending vibrations of -CH<sub>2</sub> groups at 1462 and 1362 cm<sup>-1</sup>, the stretching vibration of the cyanide group at 2254 cm<sup>-1</sup>, the stretching vibrations of aliphatic C-H at 2950

**SCHEME 1** The advance strategy for the synthesis of (PMAA-b-PAM-b-PCL-SH) triblock copolymer [Colour figure can be viewed at wileyonlinelibrary.com]



**SCHEME 2** Schematic structure of doxorubicin (DOX)-loaded PMAA-b-PAM-b-PCL-SH triblock copolymer [Colour figure can be viewed at wileyonlinelibrary.com]

and 2850 cm $^{-1}$ , and symmetric and asymmetric stretching vibrations of C-O-C group at 1176 and 1242 cm $^{-1}$ . $^{5,11}$ 

The main absorption bands in the  $(PAM-b-PCL-S)_2$  (Figure 2B) copolymer were displayed some new absorption bands including the stretching vibration of amine groups related to AM as a broad band centered at 3445 cm<sup>-1</sup> and the stretching vibration of carbonyl group at 1666 cm<sup>-1</sup>.

As demonstrated in Figures 2C, owing to overlapping of PMAA bands with the absorption bands of PAM as well as PCL sections, the FTIR spectrum of the PMAA-b-PAM-b-PCL-SH sample does not show any different band. The best significant change is the shift of carbonyl stretching vibration to lower wavelength owing to hydrogen bonding after copolymerization of MAA monomer. As shown in Figure 2D, the FTIR spectrum of the PMAA-b-PAM-b-PCL-SH triblock copolymer did not show any distinct band, in comparison with the FTIR spectrum of the (PMAA-b-PAM-b-PCL-S)2 pentablock copolymer.

The successful synthesis of (CTA-PCL-S)<sub>2</sub>, (PAM-b-PCL-S)<sub>2</sub>, (PMAA-b-PAM-b-PCL-S)<sub>2</sub>, and PMAA-b-PAM-b-PCL-SH were further verified by means of <sup>1</sup>H NMR spectroscopy as shown in Figures 3, 4, and 5. The (CTA-PCL-S)<sub>2</sub> exhibited all chemical resonance of RAFT and PCL agent as demonstrated in the <sup>1</sup>H NMR spectrum of the sample (Figure 3). The number-average molecular weight (Mn) and degree of polymerization (DPn) of the synthesized (CTA-PCL-S)<sub>2</sub> materials were deliberated from the <sup>1</sup> HNMR data by the means of subsequent equations:<sup>10</sup>

$$DP_{n,PCL} = \frac{I_d/2}{I_e/2} = 41,$$

$$\begin{split} \text{Mn, } & (\text{CTA} - \text{PCL} - \text{S})_2 = 2 \times \left[ \text{DP}_{n,\text{PCL}} \times \text{M}_{\text{CL}} \right] + 2 \times \text{M}_{\text{CTA}} \\ & + M_{\text{bis}(2\text{hydroxyethyl})\text{disulfiede}} - 2 \times \text{M}_{\text{H}_2\text{O}} = 10036. \end{split}$$

As seen in Figure 4, the  $^1$ H NMR spectrum of the (PAM-b-PCL-S) $_2$  triblock copolymer exhibited some new chemical resonance containing methine and methylene groups of PAM (f and g) at 0.80 to 2.6 ppm and amide groups of AM (h) at 6.89 to 7.96 ppm that verify the successful preparation of (PAM-b-PCL-S) $_2$  triblock copolymer. Additionally, the Mn of PAM part was planned from the  $^1$ H NMR data via the subsequent equation:

$$\begin{split} \text{Mn, } \left(\text{PAM-b-PCL-S}\right)_2 &= 2 \times \left(\text{M}_{n,\text{Macro-RAFT}} + \left[\text{DP}_{n,\text{PCL}} \times \frac{2 \times I_a}{2 \times I_h} \times 71.08\right]\right) \\ &= 2 \times (5018 + 5575) = 21186. \end{split}$$

$$M_{n,PAM} = 5575,$$

$$DP_{n,PAM} = 78.$$

Lastly, the bearing of new chemical shift at 12.35 ppm (z) associated with the hydroxyl group of carboxylic acid demonstrated the presence of PMAA in the materials. The chemical resonance of the protons of other segments was overlapped with methane and methylene groups in the polymer structure (m and n) (Figure 5). Additionally, the Mn of PMAA part was measured from the <sup>1</sup>H NMR data via the subsequent equation:

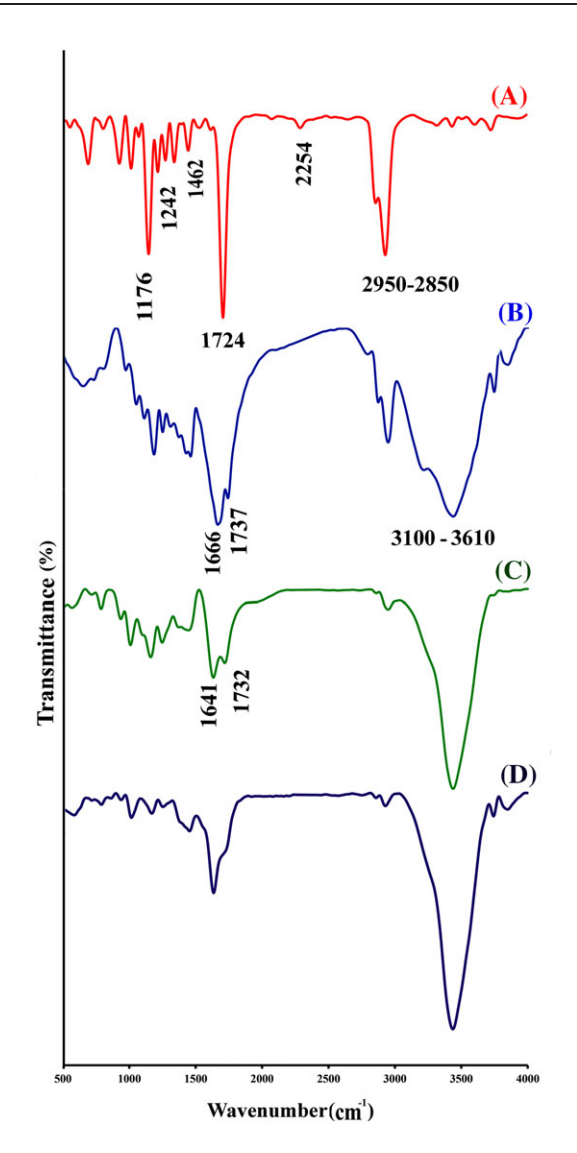


**FIGURE 2** The Fourier transform infrared (FTIR) spectra of A, (CTA-PCL-S)<sub>2</sub>; B, (PAM-b-PCL-S)<sub>2</sub>; C, (PMAA-b-PAM-b-PCL-S)<sub>2</sub>; and D, PMAA-b-PAM-b-PCL-SH [Colour figure can be viewed at wileyonlinelibrary.com]

$$\begin{split} \text{Mn, } \left( \text{PMAA-}b\text{-PAM-}b\text{-PCL-S} \right)_2 &= 2 \times \left( M_{n,\text{Macro-RAFT}} + \\ & \left[ M_{n,\text{PAM-}b\text{-PCL}} \times \frac{(I_k \times 86.06)/1}{(I_f \times 71.08)/2} \right] \right) \\ &= 2 \times (10593 + 11880) = 44947, \\ & M_{n,\text{PMAA}} = 11880, \\ & DP_{n,\text{PMAA}} = 138. \end{split}$$

## 3.1.2 | GPC analysis

The GPC chromatograms of the (PCL-S)<sub>2</sub>, (PAM-b-PCL-S)<sub>2</sub>, (PMAA-b-PAM-b-PCL-S)<sub>2</sub>, and PMAA-b-PAM-b-PCL-SH samples are shown in Figure 6. Synthesized materials displayed monomodal chromatograms that support there is no homopolymer impurity. The molecular weights gained from H NMR and GPC data were compared with each other in Table 1. As seen, synthesized materials show low dispersity (Đ) values. That demonstrated the good control over the RAFT polymerization.

## 3.2 | Evaluation of GNSs@polymer nanocarrier

## 3.2.1 | FTIR and UV-Vis spectroscopies

The FTIR spectra of the GNSs and GNSs conjugated PMAA-b-PAM-b-PCL-SH (GNPs@polymer) nanosystem are shown in Figure 7. The FTIR spectrum of GNSs demonstrated antisymmetric and symmetric stretching vibrations of carboxylate ions (corresponded to the citrate groups) on the surface of GNSs at 1589 and 1397 cm<sup>-1</sup>, respectively, the stretching vibrations of aliphatic C-H (related to citrate groups) at 2950 to 2850 cm<sup>-1</sup> region, carbonyl stretching vibration at 1719 cm<sup>-1</sup>, and surface hydroxyl groups of GNSs or adsorbed water as a broad band centered<sup>11</sup> at 3430 cm<sup>-1</sup>. The successful conjugation of GNPs with PMAA-b-PAM-b-PCL-SH triblock copolymer is established through the appearance of some new bands or significant changes in

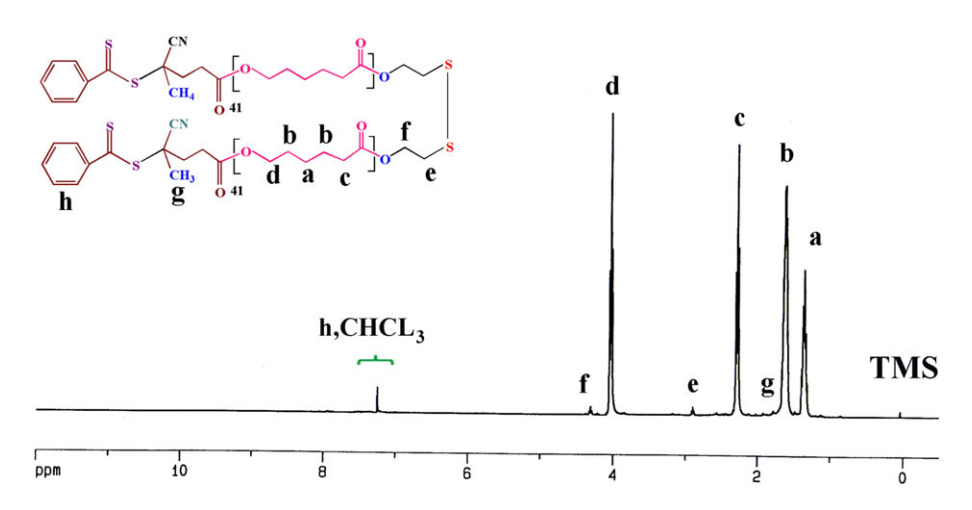


**FIGURE 3** Proton nuclear magnetic resonance (<sup>1</sup>H NMR) spectrum of (CTA-PCL-S)<sub>2</sub> macro-reversible addition-fragmentation chain transfer (RAFT) agent [Colour figure can be viewed at wileyonlinelibrary.com]

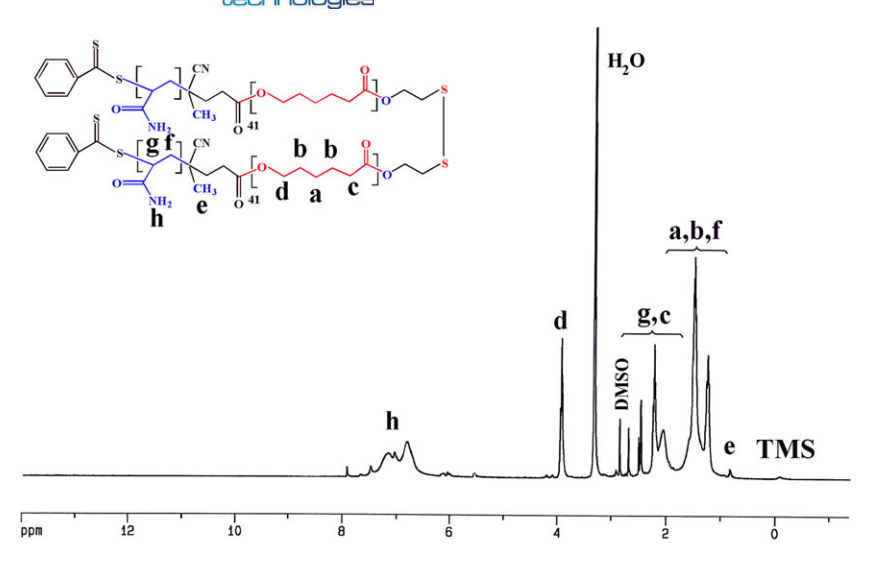


**FIGURE 4** Proton nuclear magnetic resonance (<sup>1</sup>H NMR) spectrum of (PAM-b-PCL-S)<sub>2</sub> triblock copolymer [Colour figure can be viewed at wileyonlinelibrary.com]

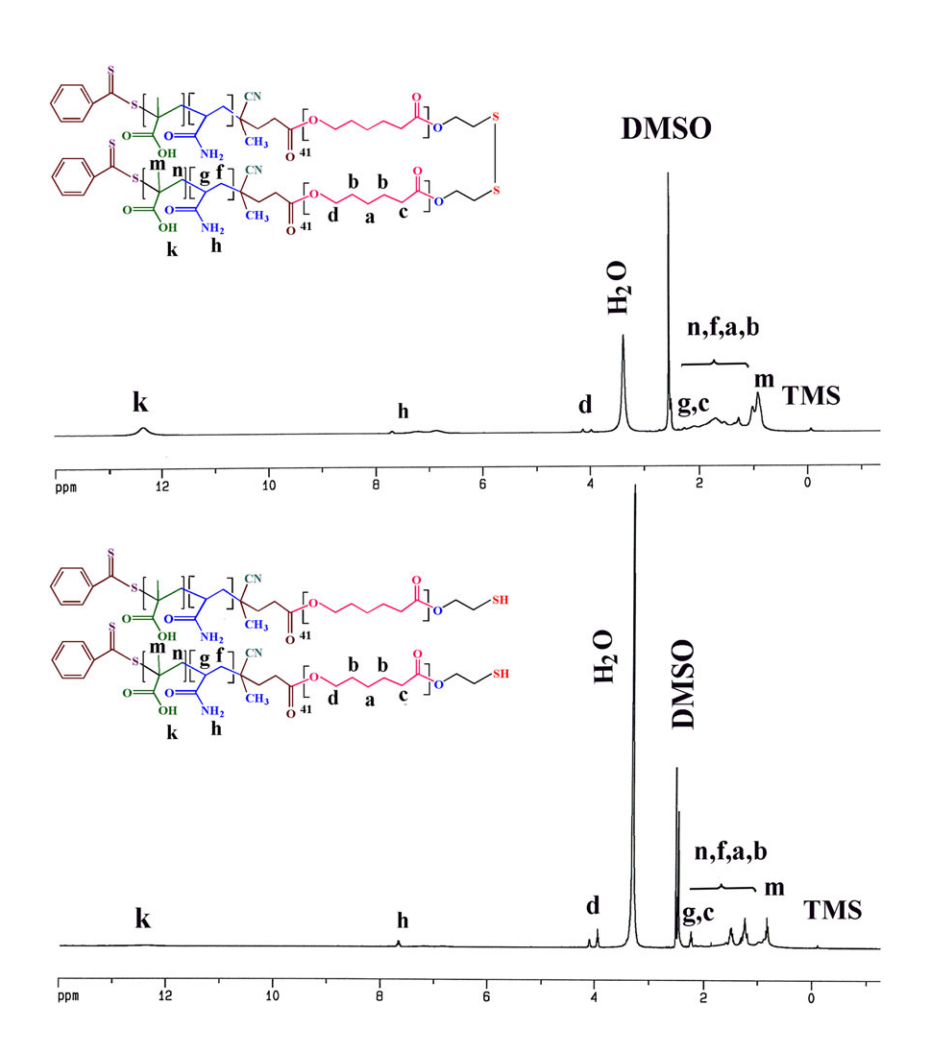


**FIGURE 5** Proton nuclear magnetic resonance (<sup>1</sup>H NMR) spectra of (PMAA-b-PAM-b-PCL-S)<sub>2</sub> pentablock copolymer and the PMAA-b-PAM-b-PCL-SH triblock copolymer [Colour figure can be viewed at wileyonlinelibrary.com]

the FTIR spectrum as follows. The FTIR spectrum of the GNSs@polymer nanocarrier displayed the stretching vibration of carbonyl groups at 1679 and 1733 cm $^{-1}$  related to PAM and PMAA segments, respectively, the stretching vibrations of C-H groups at 2927 to 3182 cm $^{-1}$  region, the bending vibrations of -CH $_2$  groups at 1433 and 1348 cm $^{-1}$ , the stretching vibration of amide and hydroxyl groups

as a broad band centered at 3367 cm<sup>-1</sup>, and asymmetric and symmetric stretching vibrations of C-O-C group at 1268 and 1139 cm<sup>-1</sup>.

As seen in Figure 8, because of surface plasmon resonance (SPR) of GNSs, the UV-Vis spectra of the GNSs and GNSs@polymer were characterized by an electronic transition at 521 and 600 nm, respectively. Furthermore, the maximum absorption peak of GNSs@polymer

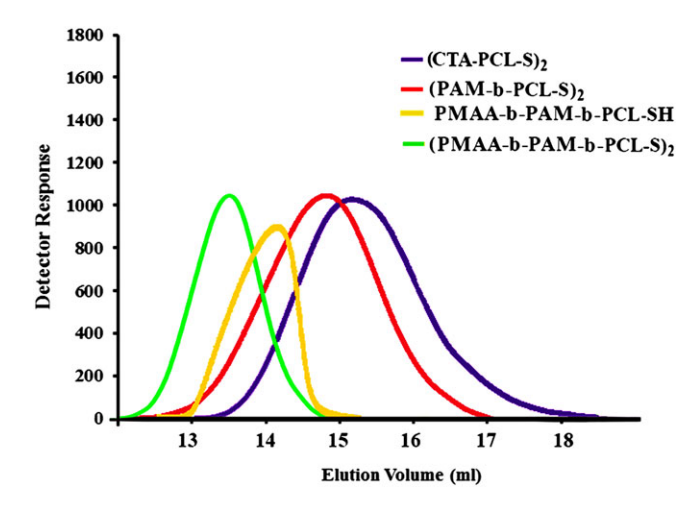


**FIGURE 6** Gel permeation chromatography (GPC) chromatograms of (CTA-PCL-S)<sub>2</sub>, (PAM-*b*-PCL-S)<sub>2</sub>, (PMAA-*b*-PAM-*b*-PCL-S)<sub>2</sub>, and PMAA-*b*-PAM-*b*-PCL-SH samples [Colour figure can be viewed at wileyonlinelibrary.com]

**TABLE 1** Molecular weight analysis data of (CTA-PCL-S)<sub>2</sub>, (PAM-b-PCL-S)<sub>2</sub>, (PMAA-b-PAM-b-PCL-S)<sub>2</sub>, and PMAA-b-PAM-b-PCL-SH samples by GPC

Sample	$M_{\rm n}^{a}$ , g mol <sup>-1</sup>	Đ <sup>a</sup>	$M_{\rm n}^{\rm b}$ , g mol <sup>-1</sup>
(CTA-PCL-S) <sub>2</sub>	13 000	1.65	10 036
(PAM-b-PCL-S) <sub>2</sub>	23 100	1.39	21 186
(PMAA-b-PAM-b-PCL-S) <sub>2</sub>	41 200	1.24	44 947
PMAA-b- PAM-b-PCL-SH	24 320	1.32	23 422

Abbreviation: GPC, gel permeation chromatography.

<sup>&</sup>lt;sup>b</sup>Calculated from proton nuclear magnetic resonance (<sup>1</sup>H NMR) data.

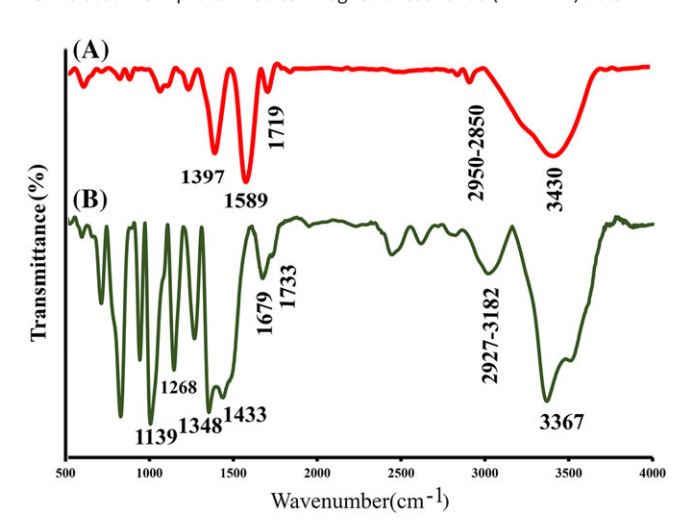


**FIGURE 7** The Fourier transform infrared spectra of the A, gold nanospheres (GNSs) and B, GNSs@polymer [Colour figure can be viewed at wileyonlinelibrary.com]

sample showed a major red shift that approve a linear growth in particle size due to the surface modification. As a result, the synthesized sample can be used for theranostic applications and chemophotothermal therapy because of optical absorption in the NIR.

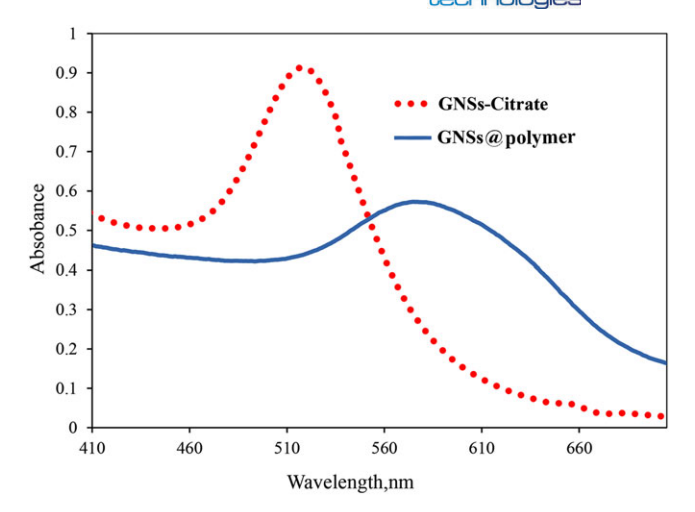


**FIGURE 8** The ultraviolet-visible (UV-Vis) spectra of the gold nanospheres (GNSs) and GNSs@polymer [Colour figure can be viewed at wileyonlinelibrary.com]

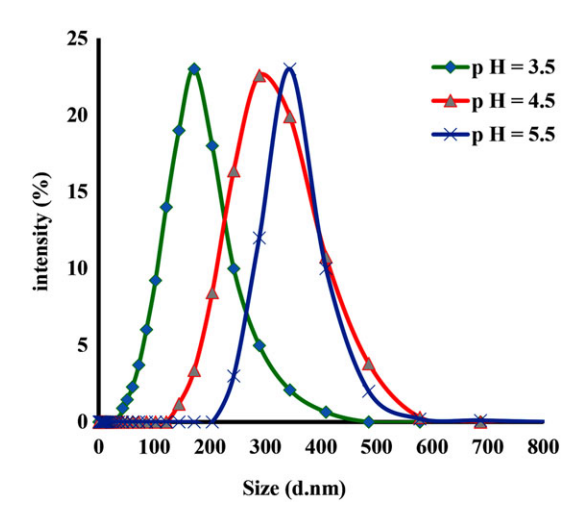


**FIGURE 9** The dynamic light scattering plots of gold nanospheres (GNSs)@polymer at various condition [Colour figure can be viewed at wileyonlinelibrary.com]

#### 3.2.2 | DLS measurement

DLS used for demonstrated self-assembly behavior of the synthesized thiol-end-capped polymer under pH stimuli (Figure 9). PMAA block can affect the size and size distribution of the micelles because the PMAA segment displays different hydrophobicity or hydrophilicity depend on the deprotonation or protonation of its carboxyl groups in various pH solutions. In acidic solutions (pH < 4.2), the PMAA, PAM, and PCL segments placed as the shell, corona, and cores of micelles, respectively. But, in higher pH values (pH > 4.2), the PMAA, PAM, and PCL segments placed as the corona, shell, and cores of micelles, respectively, owing to the deprotonation of the carboxyl groups of the PMMA segments.

As a result, when pH increased from initial 4.50 to 5.50, the mean diameters of the micelles increase from 289 to 344 nm, which was likely owing to the intramicellar increasing electrostatic repulsion between poly(methacrylic acid) outer shells, due to the deprotonation

<sup>&</sup>lt;sup>a</sup>Determined by GPC.

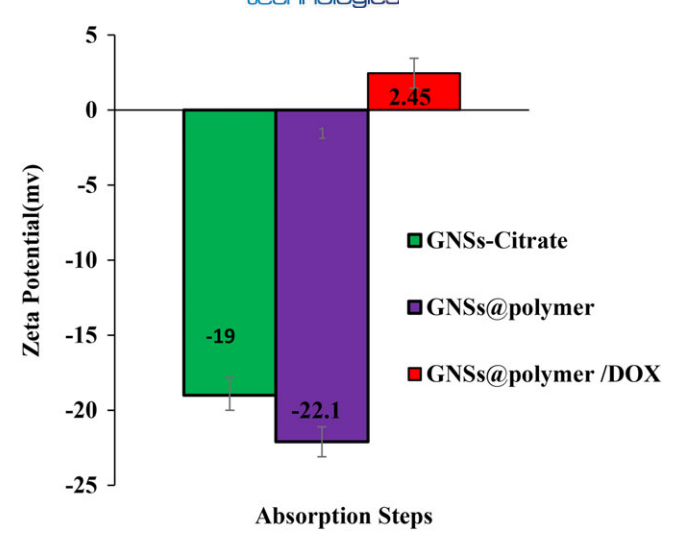


**FIGURE 10** Zeta potentials of as-prepared gold nanospheres (GNSs)-citrate, GNSs@polymer, GNSs@polymer-doxorubicin (DOX) dispersed in the aqueous solution (pH = 7.4) [Colour figure can be viewed at wileyonlinelibrary.com]

of carboxyl groups. When pH reduced from initial 4.50 to 3.50, the mean diameters of the micelles reduced from initial 289 to 171 nm, which was likely because of the hydrogen bonding within the protonated poly(methacrylic acid).<sup>5</sup>

#### 3.2.3 ∣ Zeta potential (₹)

As seen in Figure 10, generally because of the presence of negatively charged citrate moiety on the surface of nanoparticles, the zeta potential of GNSs is about –19 mV. After modification of GNSs with PMAAb-PAM-b-PCL-SH triblock copolymer, the zeta potential of nanocarriers is changed to –22.1 mV because of the negatively charged carboxyl groups of methacrylic acid in the PMAA segment. Furthermore, the negatively charged value demonstrated the successful preparation of GNSs@polymer.

GNSs@polymer-DOX nanocarrier shows many positive values (2.45 mV) because of efficient and successful loading of DOX into the developed nanocarriers. It is important to note, because of the cationic

nature of DOX (pKa = 8.3), this drug can be effectively loaded into the negatively charged GNSs@polymer via the electrostatic interactions.

#### 3.2.4 | TEM observation

The TEM image (Figure 11A) shows that the achieved GNSs had a uniform and well-defined structure with an average diameter of 15  $\pm$  5 nm. Figure 11B shows the PMAA-b-PAM-b-PCL-SH triblock copolymer were well dispersed as individual nanoparticle and spherical shape with an average diameter of approximately 35 nm, which further reason for self-assembly ability of the thiol-end-capped polymer in aqueous solutions.

Figure 11C shows the GNSs@polymer was well dispersed as individual nanoparticle with an average diameter of approximately 75 nm and can be seen the pale shadow around GNSs due to coating GNSs with the thiol-end-capped triblock copolymer (PMAA-b-PAM-b-PCL-SH).

### 3.3 | In vitro drug release study

The biodistribution and pharmacokinetics of DOX were improved by the GNSs@polymer nanomicelles developed as a nanocarrier for DDS. The main role of these nanocarriers is providing a controlled release of drugs.

DOX can be conjugated into GNSs@polymer by the subsequent reasons: (a) DOX had a positively charged in physiological condition (DOX pKa = 8.3), which created an electrostatic attraction between the anionic carboxylic group of PMAA in nanocarriers and positive charge of DOX amino groups (Figure 12) and (b) DOX can be physically loaded in the polymeric chain. Consequently, a large number of DOX molecules could be conjugated to the GNSs@polymer.

Dialysis way was used for calculating pH effects on the release of DOX from GNSs@polymer-DOX at pH = 7.4 (median value of normal physiological condition) and 4 and 5.4 (pH value of cancer cell lysosomal and endosomal). The release rate of DOX was planned by the subsequent equation:

$$R = M_1/M_0$$
,

where  $M_0$  is the total loading amount of DOX in the thiol-end-capped polymer, and  $M_1$  is the cumulative mass of DOX released from the

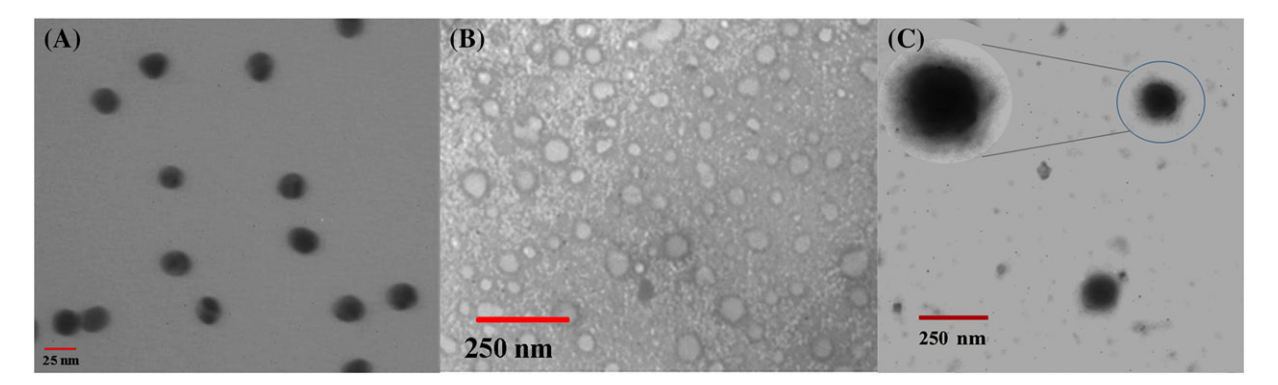


**FIGURE 11** Transmission electron microscopy (TEM) images of gold nanospheres (GNSs) of A, PMAA-b-PAM-b-PCL-SH copolymer and B, GNSs@polymer in aqueous solution [Colour figure can be viewed at wileyonlinelibrary.com]

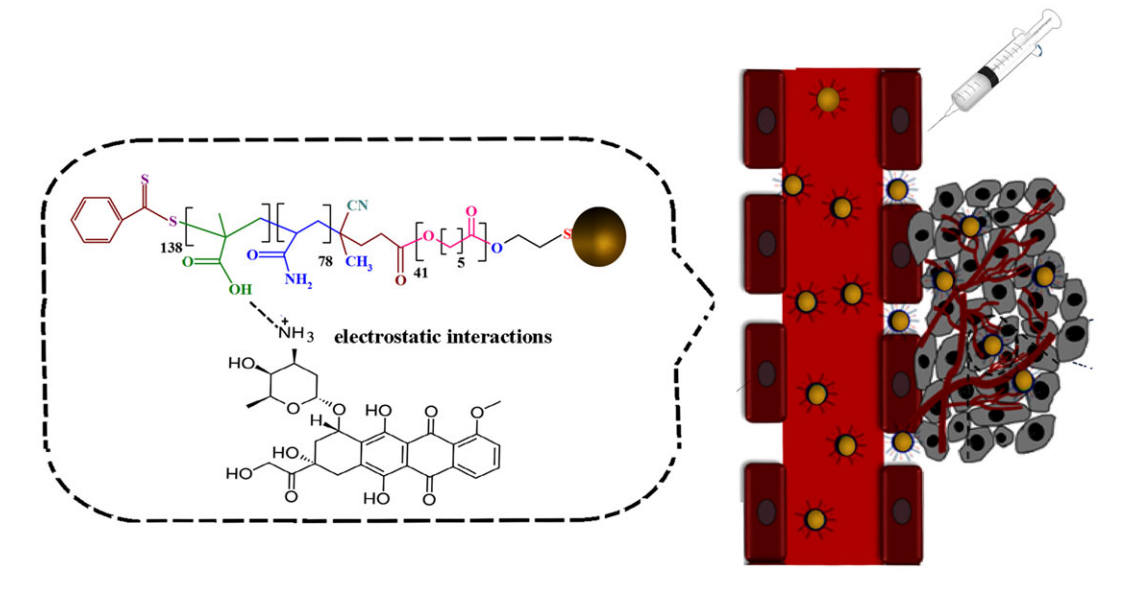


FIGURE 12 Electrostatic attraction between doxorubicin (DOX) and gold nanospheres (GNSs)@polymer at physiological conditions [Colour figure can be viewed at wileyonlinelibrary.com]

sample at a particular time. As seen in Figure 13, DOX release from GNSs@polymer is a pH-responsive process. Because, the PMAA segments was fully deprotonated at neutral pH (7.4) due to the strong interaction of DOX with thiol end-capped polymer, which delays the release of the loaded drug. In contrast, the protonation of the carboxyl group of PMAA in acidic conditions resulted in a faster dissociation of polymer-DOX complex, leading to increased release of DOX at lower pHs.

According to Figure 13, the conclusion could drown that the drug release values in pHs 4, 5.4, and 7.4 after 100 hours were 83%, 57%, and 27%, respectively.

Therefore, we concluded from the release profile that under acidic conditions (simulated cancerous tissue, pH 5.4 and 4.0), the release of DOX was faster than the physiologic condition (pH 7.4, 37°C) from the nanocarriers.

## 3.4 | Cytotoxicity tests

The biocompatibility of the blank nanocarrier (GNSs@polymer) and cytotoxic effects of the GNSs@polymer-DOX were evaluated using MTT assay against MCF7 cells (Figures 14). After 48 hours, the cell viability percentage for GNSs@polymer was over 90% even at high concentration (250 µg mL<sup>-1</sup>), representing the nanocarrier can be considered as a safe biomaterial for biomedical applications. Moreover, the cytotoxicity test showed that GNSs@polymer-DOX induced cytotoxic effects, which can be considered as an efficient anticancer drug delivery nanosystem. It should be noted that in the same concentrations of GNSs@polymer-DOX and free DOX, the higher cytotoxic effects were shown for GNSs@polymer-DOX in comparison with free DOX form.

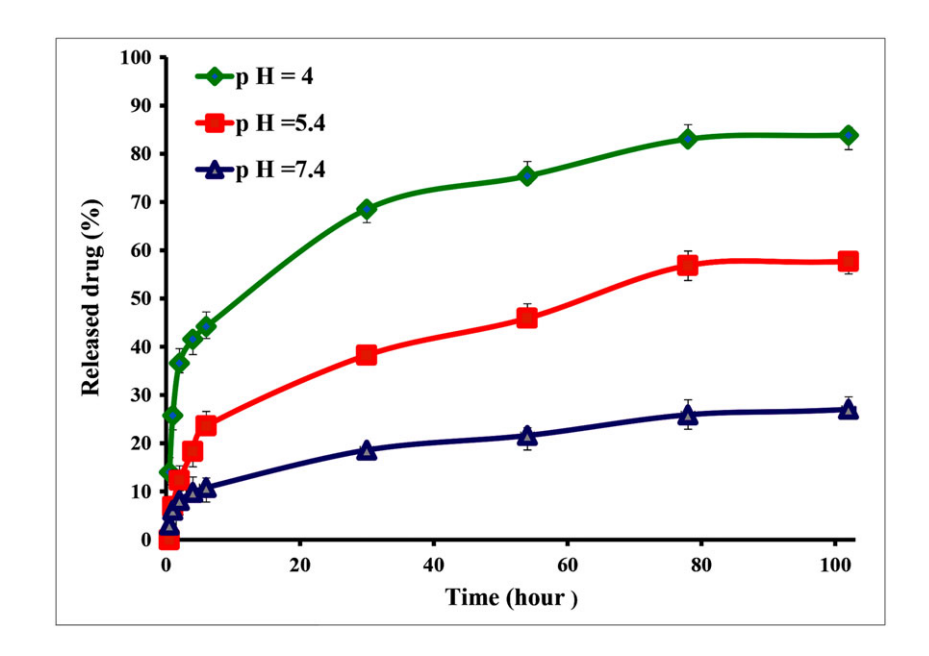


**FIGURE 13** In vitro release profiles of gold nanospheres (GNSs)@polymer-doxorubicin (DOX) at various pHs (37°C) [Colour figure can be viewed at wileyonlinelibrary.com]

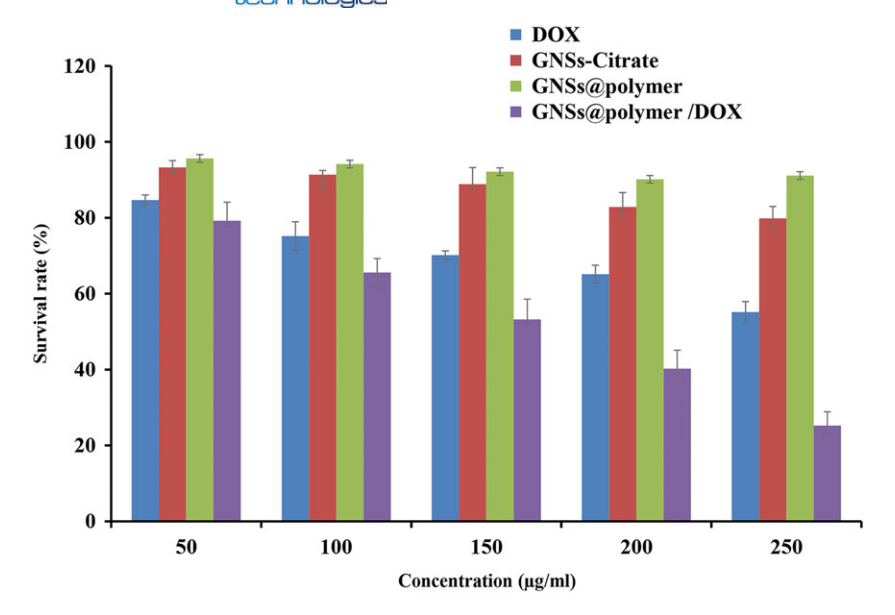


**FIGURE 14** Cell viability tests of the gold nanospheres (GNSs)-citrate, GNSs@polymer, and GNSs@polymer-doxorubicin (DOX) on MCF7 cell line [Colour figure can be viewed at wileyonlinelibrary.com]

### 4 | CONCLUSIONS

A novel pH-responsive nano-sized DDS were synthesized through the conjugation of [poly(methacrylic acid) -b-poly(acrylamide) -b-poly(εcaprolactone)-SH; PMAA-b-PAM-b-PCL-SH] triblock copolymer with GNSs followed by loading of DOX as a model anticancer drug. The molecular weight of each segment in the triblock copolymer was measured from GPC analysis and compared with those from <sup>1</sup>H NMR data results. The TEM image of GNSs demonstrated the well-defined and uniform structure with an average diameter of 15 ± 5 nm. But. GNSs@polymer showed a larger size about approximately 75 nm, which supports the successful coating of GNSs via PMAA-b-PAM-b-PCL-SH triblock copolymer. The pH sensitivity and self-assembly behavior of GNSs@polymer nanocarrier were also proved by DLS measurements. The particle size of nanocarriers at 25°C and pH values of 5.5, 4.5, and 3.5 were attained to be 344, 289, and 171 nm, respectively. This reduction in the size of nanocarrier by reducing the pH values is associated with the collapse of PMAA sections. The zeta potential of GNSs@polymer-DOX nanocarrier shows much positive value (2.45 mV) because of efficient and successful loading of DOX into the developed nanocarrier. The DOX loading capacity of the synthesized nanocarrier was calculated to be 94.63% using UV-Vis spectroscopy. The drug release GNSs@polymer-DOX demonstrated that a high drug release process at cancerous conditions (pH 5.4 and 4.0) while a low drug release value in physiological conditions (pH 7.4). The biocompatibility of the GNSs@polymer and polymer was confirmed through the MTT assay against the MCF7 cell line.

As a result, the synthesized nanocarrier (GNSs@polymer-DOX) can be used as *a de novo* DDS for chemo-photothermal therapy and theranostic applications because of smart behavior and physicochemical features such as pH sensivity and optical absorption in the NIR.

#### **ACKNOWLEDGEMENTS**

The author expresses their gratitude to the Tabriz University of Medical Sciences and Tehran Halal Research Center for supporting this project.

#### **ORCID**

Farideh Mahmoodzadeh https://orcid.org/0000-0002-7354-3466

#### **REFERENCES**

- Zimmermann S, Dziadziuszko R, Peters S. Indications and limitations of chemotherapy and targeted agents in non-small cell lung cancer brain metastases. Cancer Treat Rev. 2014;40(6):716-722.
- Ghorbani M, Mahmoodzadeh F, Nezhad-Mokhtari P, Hamishehkar H.
   A novel polymeric micelle-decorated Fe <sub>3</sub> O <sub>4</sub>/Au core-shell nanoparticle for pH and reduction-responsive intracellular co-delivery of doxorubicin and 6-mercaptopurine. New J Chem. 2018;42(22):18038-18049.
- Ghorbani M, Hamishehkar H. A novel multi stimuli-responsive PEGylated hybrid gold/nanogels for co-delivery of doxorubicin and 6mercaptopurine. Mater Sci Eng C. 2018;92:599-611.
- Abbasian M, Roudi MM, Mahmoodzadeh F, Eskandani M, Jaymand M. Chitosan-grafted-poly (methacrylic acid)/graphene oxide nanocomposite as a pH-responsive de novo cancer chemotherapy nanosystem. *Int J Biol Macromol*. 2018;118(Pt B):1871-1879.
- Mahmoodzadeh F, Abbasian M, Jaymand M, Amirshaghaghi A. A novel dual stimuli-responsive thiol-end-capped ABC triblock copolymer: synthesis via reversible addition-fragmentation chain transfer technique, and investigation of its self-assembly behavior. *Polym Int*. 2017;66(11):1651-1661.
- Lee ES, Na K, Bae YH. Polymeric micelle for tumor pH and folatemediated targeting. J Control Release. 2003;91(1-2):103-113.
- Lale SV, Koul V. Stimuli-responsive polymeric nanoparticles for cancer therapy. In: *Polymer Gels*. Singapore: Springer; 2018:27-54.
- Lim EK, Chung B, Chung S. Recent advances in PH-sensitive polymeric nanoparticles for smart drug delivery in cancer therapy. Curr Drug Targets. 2016;17(999):1-1.

- Sugihara S, Kanaoka S, Aoshima S. Stimuli-responsive ABC triblock copolymers by sequential living cationic copolymerization: multistage self-assemblies through micellization to open association. *J Polym Sci Part A Polym Chem.* 2004;42(11):2601-2611.
- Sofla SF, Abbasian M, Mirzaei M. Synthesis and micellar characterization of novel pH-sensitive thiol-ended triblock copolymer via combination of RAFT and ROP processes. Int J Polym Mater Po. 2018;68:1-11.
- Abbasian M, Judi M, Mahmoodzadeh F, Jaymand M. Synthesis and characterization of a pH-and glucose-responsive triblock copolymer via RAFT technique and its conjugation with gold nanoparticles for biomedical applications. *Polym Adv Technol.* 2018:29(12):3097-3105.
- Klaikherd A, Nagamani C, Thayumanavan S. Multi-stimuli sensitive amphiphilic block copolymer assemblies. J Am Chem Soc. 2009:131(13):4830-4838.
- Canning SL, Smith GN, Armes SP. A critical appraisal of RAFT-mediated polymerization-induced self-assembly. *Macromolecules*. 2016;49(6): 1985-2001.
- Zhou C, Hillmyer MA, Lodge TP. Efficient formation of multicompartment hydrogels by stepwise self-assembly of thermoresponsive ABC triblock terpolymers. J Am Chem Soc. 2012;134(25):10365-10368.
- Chang C, Wei H, Feng J, Wang Z. Temperature and pH double responsive hybrid cross-linked micelles based on P (NIPAAm-co-MPMA)-b-P (DEA): RAFT synthesis and "schizophrenic." micellization. *Macromolecules*. 2009;42(13):4838-4844.
- Chen J, Liu M, Gong H, Huang Y, Chen C. Synthesis and self-assembly of thermoresponsive PEG-b-PNIPAM-b-PCL ABC triblock copolymer through the combination of atom transfer radical polymerization, ring-opening polymerization, and click chemistry. J Phys Chem B. 2011;115(50):14947-14955.
- Liao ZS, Huang SY, Huang JJ, et al. Self-assembled PH-responsive polymeric micelles for highly efficient, noncytotoxic delivery of doxorubicin chemotherapy to inhibit macrophage activation: in vitro investigation. *Biomacromolecules*. 2018;19(7):2772-2781.
- Taillefer J, Jones MC, Brasseur N, Van Lier JE, Leroux JC. Preparation and characterization of PH-responsive polymeric micelles for the delivery of photosensitizing anticancer drugs. J Pharm Sci. 2000;89(1):52-62.
- Abbasian M, Mahmoodzadeh F. Synthesis of chitosan-graft-poly (acrylic acid) using 4-Cyano-4- [(phenylcarbothioyl) sulfanyl] pentanoic acid to serve as RAFT agent synthesis of chitosan-graft-poly (acrylic acid) using 4-cyano-4- [(phenylcarbothioyl) sulfanyl] Pentanoic. *J Polym Mater.* 2016;32:527-541.
- Abbasian M, Mahmoodzadeh F. Synthesis of antibacterial silver-chitosanmodified bionanocomposites by RAFT polymerization and chemical reduction methods. J Elastomers Plast. 2017;49(2):173-193.
- Abbasian M, Ghaeminia H, Jaymand M. A facile and efficient strategy for the functionalization of multiple-walled carbon nanotubes using well-defined polypropylene-grafted polystyrene. *Appl Phys Mater Sci Process*. 2018:124(8):522.
- Babin J, Lepage M, Zhao Y. "Decoration" of shell cross-linked reverse polymer micelles using ATRP: a new route to stimuli-responsive nanoparticles. *Macromolecules*. 2008;41(4):1246-1253.
- 23. Perrier S. 50th anniversary perspective: RAFT polymerization—a user guide. *Macromolecules*. 2017;50(19):7433-7447.
- Hawker CJ, Bosman AW, Harth E. New polymer synthesis by nitroxide mediated living radical polymerizations. *Chem Rev.* 2001;101(12): 3661-3688.
- Karaj-Abad SG, Abbasian M, Jaymand M. Grafting of poly[(methyl methacrylate)-block-styrene] onto cellulose via nitroxide-mediated polymerization, and its polymer/clay nanocomposite. *Carbohydr Polym*. 2016:152:297-305.

- Abbasian M, Pakzad M, Nazari K. Synthesis of cellulose-graftpolychloromethylstyrene-graft-polyacrylonitrile terpolymer/organoclay bionanocomposite by metal catalyzed living radical polymerization and solvent blending method. *Polym-Plast Technol Eng.* 2017;56(8):857-865.
- Sun JT, Hong CY, Pan CY. Recent advances in RAFT dispersion polymerization for preparation of block copolymer aggregates. *Polymer Chemistry*. 2013;4(4):873-881.
- Abbasian M, Mahmoodzadeh F, Salehi R, Amirshaghaghi A. Chemophotothermal therapy of cancer cells using gold nanorod-cored stimuli-responsive triblock copolymer. New J Chem. 2017;41(21):12777-12788.
- Khalilzadeh B, Charoudeh HN, Shadjou N, et al. Ultrasensitive caspase-3 activity detection using an electrochemical biosensor engineered by gold nanoparticle functionalized MCM-41: its application during stem cell differentiation. Sens Actuators B. 2016:231:561-575.
- Murphy CJ, Gole AM, Stone JW, et al. Gold nanoparticles in biology: beyond toxicity to cellular imaging. Acc Chem Res. 2008;41(12):1721-1730.
- Giljohann DA, Seferos DS, Daniel WL, Massich MD, Patel PC, Mirkin CA. Gold nanoparticles for biology and medicine. *Angew Chem Int Ed.* 2010;49(19):3280-3294.
- Huang X, Kang B, Qian W, et al. Comparative study of photothermolysis of cancer cells with nuclear-targeted or cytoplasmtargeted gold nanospheres: continuous wave or pulsed lasers. *J Biomed Opt.* 2010;15(5):058002.
- Mahmoodzadeh F, Abbasian M, Jaymand M, Salehi R, Bagherzadeh-Khajehmarjan E. A novel gold-based stimuli-responsive theranostic nanomedicine for chemo-photothermal therapy of solid tumors. *Mater Sci Eng C*. 2018;93:880-889.
- 34. Sabzichi M, Mohammadian J, Ghorbani M, et al. Fabrication of all-trans-retinoic acid-loaded biocompatible precirol: a strategy for escaping dose-dependent side effects of doxorubicin. Colloids Surf B Biointerfaces. 2017;159:620-628.
- Mahmoodzadeh F, Jannat B, Ghorbani M. Chitosan-based nanomicelle as a novel platform for targeted delivery of methotrexate. Int J Biol Macromol. 2019;126:517-524.
- 36. Ghorbani M, Hamishehkar H, Arsalani N, Entezami AA. Surface decoration of magnetic nanoparticles with folate-conjugated poly(N-isopropylacrylamide-co-itaconic acid): a facial synthesis of dual-responsive nanocarrier for targeted delivery of doxorubicin. Int J Polym Mater Polym Biomater. 2016;65(13):683-694.
- 37. Ghorbani M, Hamishehkar H. Decoration of gold nanoparticles with thiolated PH-responsive polymeric (PEG-b-p(2-dimethylamio ethyl methacrylate-co-itaconic acid)) shell: a novel platform for targeting of anticancer agent. *Mater Sci Eng C*. 2017;81:561-570.
- 38. Ma Y, Bian X, He L, Cai M, Xie X, Luo X. Immobilization of poly (acrylamide) brushes onto poly (caprolactone) surface by combining ATRP and "click" chemistry: synthesis, characterization and evaluation of protein adhesion. *Appl Surf Sci.* 2015;329:223-233.

How to cite this article: Mahmoodzadeh F, Hosseinzadeh M, Jannat B, Ghorbani M. Fabrication and characterization of gold nanospheres-cored pH-sensitive thiol-ended triblock copolymer: A smart drug delivery system for cancer therapy. *Polym Adv Technol.* 2019;30:1344–1355. <a href="https://doi.org/10.1002/pat.4567">https://doi.org/10.1002/pat.4567</a>